

A-site-disorder-dependent percolative transport and Griffiths phase in doped manganites

N. Rama and M. S. Ramachandra Rao*

Materials Science Research Centre and Department of Physics, Indian Institute of Technology-Madras, Chennai, India 600 036

V. Sankaranarayanan

Department of Physics, Indian Institute of Technology-Madras, Chennai, India 600 036

P. Majewski, S. Gepraegs, M. Opel, and R. Gross

Walther-Meissner Institute, Bavarian Academy of Sciences, Walther-Meissner Strasse, 8, D-85748 Garching, Germany

(Received 23 May 2004; revised manuscript received 18 August 2004; published 20 December 2004)

The influence of A site disorder on the magnetic and transport properties of $\text{Pr}_{0.6}\text{R}_{0.1}\text{Sr}_{0.3}\text{MnO}_3$ ($R=\text{Tb}$, Y , Ho , and Er) polycrystalline samples is analyzed within the context of percolative transport and the existence of the Griffiths phase. The temperature dependence of the average spin moment at the hopping sites and the fraction of metallic clusters bear signatures of the onset of the Griffiths phase. Our analysis suggests that the paramagnetic phase comprises of insulating correlated spin clusters that coexist with ferromagnetic metallic clusters and paramagnetic spins. This coexistence was found to be sensitive to the A-site disorder.

DOI: 10.1103/PhysRevB.70.224424

PACS number(s): 75.47.Lx, 64.60.Ak

Over the last decade, there has been an intense experimental and theoretical effort to understand the complex physics of the perovskite type doped manganites of composition $R_{1-x}A_x\text{MnO}_3$ with $R=\text{La}$, Pr , Nd , etc. and $A=\text{Ca}$, Sr , and Ba .¹ The prototypical simultaneous transition from a paramagnetic insulating to a ferromagnetic metallic state in this material class is usually described within the framework of the double exchange mechanism proposed by Zener² in which the mobile $3d e_g$ electrons of the Mn^{3+} ions couple ferromagnetically to the core localized $3d t_{2g}$ spins due to a strong Hund's coupling. However, calculations to account for large changes in resistivity within this framework did not yield satisfactory results.³ It became evident that a localization mechanism not considered by the double exchange model is necessary to explain the large magnetic field and temperature dependence of the resistivity observed in experiments.³ Meanwhile, there is evidence from both experiments⁴ and theoretical calculations⁵ that polaron formation due to a strong Jahn-Teller interaction plays a major role to understand the underlying physics in these materials.

From small angle neutron scattering combined with measurements of the volume thermal expansion and the magnetic susceptibility, De Teresa *et al.*⁶ found that ferromagnetic clusters exist above the Curie temperature, T_C . Furthermore, Raman spectroscopy studies⁷ provided evidence for the presence of polarons below T_C as a result of strong electron phonon coupling. Finally, scanning tunneling microscopy measurements performed on $\text{La}_{0.7}\text{Ca}_{0.3}\text{MnO}_3$ films at temperatures just below T_C provide additional evidence for the coexistence of conducting and insulating clusters.⁸ The cluster size was found to increase with the increase in magnetic field suggesting that the ferromagnetic clusters above T_C are metallic. These experimental results suggest that the metal-insulator transition is a gradual process, in which over an extended temperature range around T_C there is a competition between the double exchange mechanism, which tends to delocalize charge carriers in order to maximize the kinetic

energy gain, and the electron-phonon coupling, which tends to localize the carriers.⁹ Along this line the metal-insulator transition can be thought to occur due to percolation of ferromagnetic metallic clusters.

Griffiths¹⁰ considered a percolation like problem in his paper on random Ising ferromagnets, in which only a fraction of the lattice sites are occupied by magnetic atoms and the rest are either vacant or occupied by a nonmagnetic atoms with a nearest neighbor ferromagnetic interaction existing between the magnetic atoms. When all the magnetic atoms are present, the transition occurs at a temperature T_G called the Griffiths temperature. However when the fraction of nonmagnetic atoms or vacant sites is nonzero, the transition is suppressed to a lower temperature T_C above which the free energy and magnetization was found to diverge. This was attributed to the accumulation of clusters whose local transition temperatures were found to exceed T_C . Bray and Moore^{11,12} extended this argument to all systems in which disorder suppresses the magnetic transition from its pure value T_G to T_C . Such a system was found to exhibit a sharp downturn in the inverse of high temperature susceptibility before T_C . The temperature range between the pure transition temperature T_G and T_C was termed as Griffiths phase. When the fraction of the magnetic atoms is less than a critical concentration called the percolation threshold, there is no spontaneous magnetization. In the case of manganites, the fraction of ferromagnetically interacting regions is equivalent to the fraction of metallic regions assuming the double exchange model is correct. Thus there exists a corresponding percolation threshold for metallic behavior.

Griffiths theory predicts that above the ferromagnetic transition temperature T_C in a system with randomly distributed spins, there is always a finite probability of finding an arbitrary large ferromagnetic cluster. Such a system exhibits a sharp downturn in the inverse of the high temperature magnetic susceptibility above T_C . A similar behavior was seen in $\text{La}_{0.7}\text{Ca}_{0.3}\text{MnO}_3$ by De Teresa *et al.*⁶ and was explained re-

cently by Salamon *et al.*¹³ using the Griffith's model. There are several factors affecting percolation effects in the doped manganites. Among these the most prominent are the average ionic radius of the *A*-site cation, variance of the *A*-site disorder, oxygen deficiency, epitaxial strain, or grain boundary effects. It is well known that the para- to ferromagnetic and insulator to metal transition temperatures in the perovskite type doped manganites depend on doping, i.e. on the amount of substitution of the trivalent *A*-site cation by a divalent alkaline earth element. However, the magnetic and transport properties are also significantly changed¹⁴ when the trivalent ion (e.g., La) at the *A*-site in the ABO_3 perovskite structure is substituted by other trivalent rare earth ions or Y^{3+} . A random distribution of *A*-site cations of different ionic radii results in a random tilt and distortion of the MnO_6 octahedra.¹⁵ This, in turn, leads to a reduction of the hopping matrix element of the e_g electrons thereby narrowing the effective electronic bandwidth.¹⁶

In this work, we address the hitherto unaddressed issue of how the transport properties of the doped manganites are correlated to the existence of a Griffiths phase. This is also the first attempt to analyze the properties of Pr based manganites within the context of a Griffiths phase. Furthermore, we also discuss in detail how percolative transport in manganites evolves when the *A*-site disorder is increased. These questions are addressed by analyzing the magnetotransport properties of $Pr_{0.6}R_{0.1}Sr_{0.3}MnO_3$ with $R=Tb$ (PTSMO), Y (PYSMO), Ho (PHSMO), and Er (PESMO). Polycrystalline samples of $Pr_{0.6}R_{0.1}Sr_{0.3}MnO_3$ with $R=Tb$, Y , Ho , and Er were prepared using the conventional solid state method and their phase purity was checked using x-ray diffraction. The electrical transport properties of the samples were measured as a function of temperature (2–400 K) and applied magnetic field (–7 to +7 T) using the standard linear four-probe technique in an Oxford continuous flow cryostat. Field cooled magnetization measurements were carried out on powdered samples using a SQUID magnetometer (Quantum design MPMS XL) in the same temperature range in a field of 1000 Oe.

The temperature dependence of the magnetization of the samples is shown in Fig. 1. The Curie temperature T_C is found to decrease with increasing variance $\langle\sigma^2\rangle$ of the ionic radius at the *A*-site (Table I). Fits of the magnetic susceptibility to a Curie-Weiss law above T_C yield a high effective Bohr magneton number P_{eff} listed in Table I. The magnetization value at a field of 7 T and at temperature 5 K is given in brackets in Table I for comparison. It is seen that the P_{eff} values are higher than the expected spin only value of $3.7 \mu_B/fu$. The corresponding value of C , the Curie constant is also listed in Table I. It is seen that in all the four samples the Curie constant is higher than the expected C value of 2.64 (corresponding to $0.7 Mn^{3+} S=2$ and $0.3 Mn^{4+} S=1.5$). This implies that paramagnetic spin clusters are present above T_C . Since the Curie constant is twice the value expected for a Sr concentration of 0.3, it could mean that Mn ions exist as dimers. ESR linewidth studies above T_C in manganite samples with similar concentration namely $La_{0.7}Ca_{0.3}MnO_3$ suggests the possibility of the formation of $Mn^{3+}-Mn^{4+}$ spin clusters in the paramagnetic state.¹⁷ These

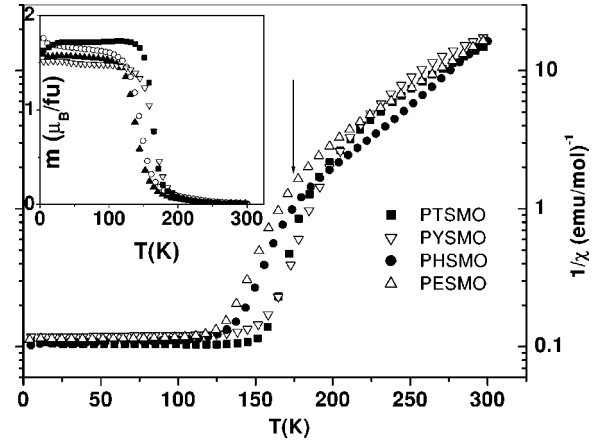


FIG. 1. Temperature variation of inverse of susceptibility for $Pr_{0.6}R_{0.1}Sr_{0.3}MnO_3$ with $R=Tb$, Y , Ho , and Er in logarithmic scale. Arrow indicates the onset of the Griffiths phase. Inset shows the magnetization taken in field cooling mode in a field of 1000 Oe.

dimers could be of the form $Mn^{3+}-O-Mn^{4+}$, the Zener pairs, which are responsible for ferromagnetism in the manganites.² The influence of these clusters is best seen by plotting $1/\chi$ in a logarithmic scale versus temperature (Fig. 1). The temperature at which a kink or a sharp downturn is seen in the plot (indicated by arrow) can be attributed to the temperature, at which the clusters begin to form and can be considered as the temperature T_G that marks the onset of the Griffiths phase.

The magnetic field dependence of the resistance both above and below T_C was analyzed using the model proposed by Wagner *et al.*¹⁸ According to this model, there is an additional activation energy present in the hopping barrier due to the magnetic field which depends on the local magnetization vectors at the hopping sites ($\Delta W_{i,j} \propto \mathbf{M}_i \cdot \mathbf{M}_j$). The magnetoresistance was found to be proportional to this magnetic barrier contribution. $M_{i,j}$ consists of two components—one due to the Weiss magnetization (M_W) and the other due to the difference between the Weiss magnetization and the saturation magnetization ($|\delta M_{i,j}| = |M_S - M_W|_{i,j}$). Wagner *et al.* show that in the paramagnetic state the magnetoresistance scales as square of the Brillouin function $B(gK\mu_B H/k_B T)$ and as the Brillouin function in the ferromagnetic state. Here, H is the applied magnetic field, $g=2$ and $K(T)$ gives the average spin moment at the hopping sites. $K(T)$ decreases below T_C since

TABLE I. Variance $\langle\sigma^2\rangle$ of the *A*-site ionic radius, Curie temperature T_C , effective Bohr magneton number P_{eff} , Curie constant and percolation threshold p_c for the investigated samples. The magnetic moment/fu at 5 K in a field of 7 T is listed in brackets for comparison sake.

| Sample | $\langle\sigma^2\rangle$ (10^{-3} \AA^2) | T_C (K) | P_{eff} μ_B/fu | C emu K mol^{-1} | p_c |
|--------|---|--------------|--------------------------------|--------------------------------|-------|
| PTSMO | 4.921 | 165 | 6.93 (4.57) | 6.02 | 0.47 |
| PYSMO | 5.394 | 164 | 6.69 (3.90) | 5.61 | 0.48 |
| PHSMO | 5.445 | 145 | 5.76 (4.67) | 4.16 | 0.51 |
| PESMO | 5.755 | 136 | 5.81 (4.62) | 4.31 | 0.58 |

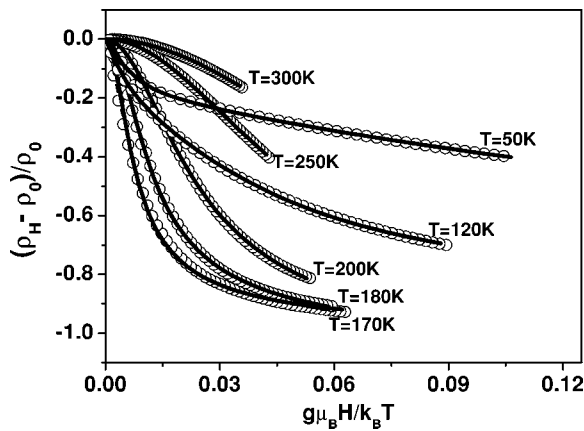


FIG. 2. Resistivity versus applied field of $\text{Pr}_{0.6}\text{Ho}_{0.1}\text{Sr}_{0.3}\text{MnO}_3$ with $T_C=145$ K at different temperatures. The symbols represent the data while the lines are fits to the square of the Brillouin function (for $T=300$ K, 250 K, 200 K, 180 K, 170 K) and to the Brillouin function (for $T=120$ K and 50 K).

$|\delta M_{i,j}| \rightarrow 0$ as $T \rightarrow 0$. The fit of the magnetoresistance data of the PHSMO sample to this function is shown in Fig. 2.

The values of K obtained by fitting the data as shown in Fig. 2 for all investigated samples are plotted along with $(1/\chi)$ versus temperature (T) in Fig. 3. It is evident from Fig. 3 that for all four samples the maximum of K does not coincide with the Curie temperature T_C but lies slightly above it. The maximum in K is seen to coincide with the temperature, where the kink is seen in the $1/\chi$ (logarithmic scale) versus T plot, i.e., to T_G . This implies that the onset of long range ordering starts at T_G itself though the ordering is fully achieved only at T_C . Thus this temperature T_G can be thought of as the Griffiths temperature where transition would have taken place if there was no disorder in the system. Below T_C , the temperature variation of K and hence long range spin ordering was found to be more gradual as the A -site disorder increases.

The magnetization and magnetoresistance data of the investigated samples give evidence for the existence of ferromagnetic clusters above T_C suggesting that there is a coex-

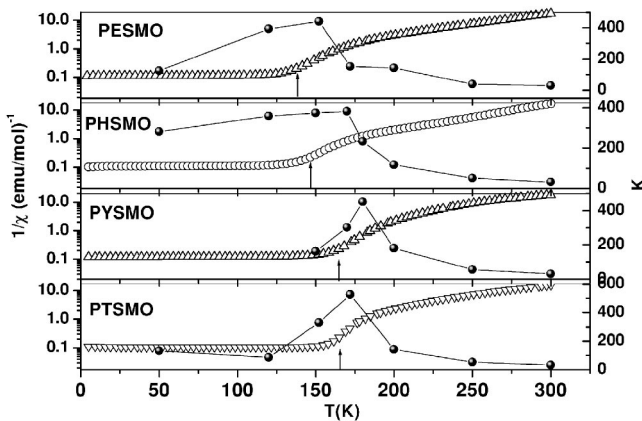


FIG. 3. Temperature dependence of K and $(1/\chi)$ (logarithmic scale) for the investigated samples. The downward arrows mark the Griffiths temperature T_G , whereas the upward arrows point to T_C .

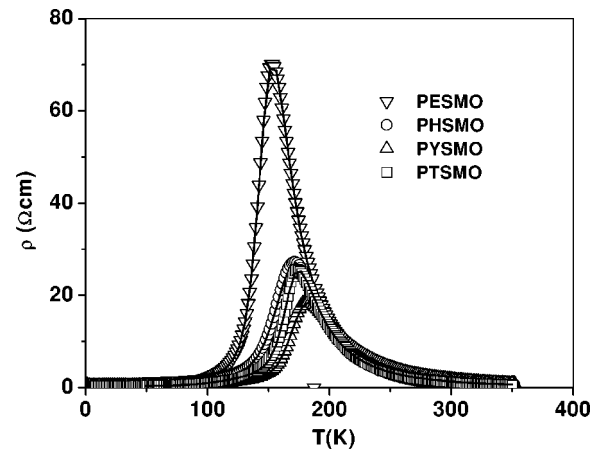


FIG. 4. Zero field resistivity versus temperature curves plots for $\text{Pr}_{0.6}\text{R}_{0.1}\text{Sr}_{0.3}\text{MnO}_3$ with $R=\text{Tb}$, Y , Ho , and Er . The symbols represent the data while the lines represent fits to the percolation model.

istence of metallic and insulating clusters in the investigated samples. Hence the temperature dependence of the resistance can be modeled as a random resistor network each consisting of a paramagnetic region “PM” sandwiched between adjacent ferromagnetic “FM” regions. Thus, the total resistance of the system comprises of two components R_{FM} and R_{PM} . The first is due to the metallic/ferromagnetic regions, whereas the latter is due to the insulating/paramagnetic regions. Hence, the total resistance of the system can be expressed as $R=pR_{\text{FM}}+(1-p)R_{\text{PM}}$, where p and $(1-p)$ are the volume fractions of the ferromagnetic/metallic and paramagnetic/insulating regions, respectively. Upon cooling the sample, the size of the metallic regions grows at the expense of the insulating regions. Therefore, a temperature dependent volume fraction p is required to fit the experimental data. On decreasing the temperature the value of p increases until a critical value p_c , the percolation threshold, where these metallic regions form a metallic percolation across the whole sample. That is, at $p=p_c$ a metallic path is formed leading to an insulator to metal transition. This is expected to occur around $T=T_C$. We have used $p=1/[1+\exp(-U/k_B T)]$ with the activation energy $U=U_0(1-T/T_C)$ to model the temperature dependence¹⁹ of p . The low temperature regime (R_{FM}) was analyzed using $\rho(T) \propto T^2 + T^{4.5}$ dependence²⁰ and in high temperature regime (R_{PM}), a temperature dependence according to the adiabatic polaron model²¹ i.e., $\rho=\rho_0 T \exp(E_A/k_B T)$ was used. The fits to the percolation equation are shown in Fig. 4.

The temperature derivative of the volume fraction p obtained by fitting the data to the percolation model is plotted in Fig. 5 along with the temperature dependence of the inverse of susceptibility. It is evident that the onset of metallicity ($p \geq p_c$) does not coincide with T_C (marked by upward arrow in Fig. 5) but occurs at a higher temperature T_G (marked by downward arrow in Fig. 5). In order to clearly illustrate these correlations the corresponding data for the PHSMO sample alone is plotted in Fig. 6. At T_G , there is a maximum in the temperature derivative of p . Though the bulk of the sample becomes ferromagnetic only at T_C , the onset starts at T_G itself as seen from Fig. 3. Since magnetism

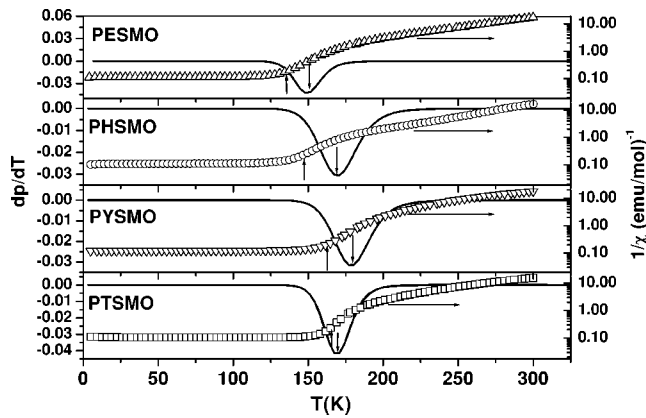


FIG. 5. Temperature dependence of the inverse of susceptibility (symbols) and the temperature derivative of metallic volume fraction p (solid lines). Upward arrow points to T_C and the downward arrow to T_G .

is correlated with metallicity in the case of manganites, a metallic short is created due to which a metal-insulator transition takes place at T_G itself and not at T_C as expected. The value of percolation threshold p_c obtained from the value of p where dp/dT shows a minimum, is found to increase with increase in A -site disorder (Table I). From Fig. 5 it is also seen that the difference between T_G and T_C increases with increase in variance of the ionic radii at the A -site indicative of a reduction in the percolation of ferromagnetic (metallic) clusters. This, along with the observation of increase of p_c with $\langle\sigma^2\rangle$ suggests that there must be an additional mechanism that comes into play because of the increase in the A -site disorder. This may be due to an increase in the localization centers in the lattice which increase with $\langle\sigma^2\rangle$ possibly resulting in the formation of insulating spin clusters that coexist with the ferromagnetic clusters above T_C . This suggestion is supported by the recent observation of correlated nanoclusters with CE-type charge/orbital order (hence insu-

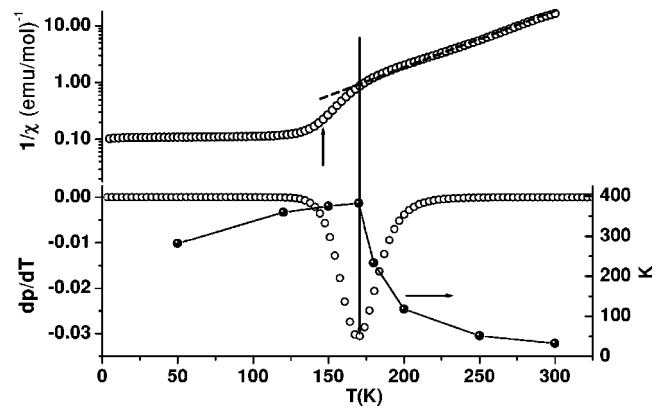


FIG. 6. Temperature dependence of the inverse of susceptibility (symbols) in logarithmic scale and the temperature derivative of metallic volume fraction p (solid lines) and k for the PHSMO sample. Upward arrow points to T_C and the downward arrow to T_G . The dotted line is a guide to the eye.

lating) from synchrotron measurements in many manganites.²²

In summary, we have systematically studied the influence of variance of the atomic radii at the A -site on the magnetotransport properties of $\text{Pr}_{0.6}\text{R}_{0.1}\text{Sr}_{0.3}\text{MnO}_3$ with $R=\text{Tb, Y, Ho, and Er}$. These properties have been interpreted within the context of percolative transport and the existence of a Griffith phase. The temperature dependence of the average spin moment at the hopping sites from the magnetoresistance data and the fraction of metallic clusters from the resistivity plots bear signatures of the onset of the Griffith phase. Our analysis suggests that the paramagnetic phase comprises of insulating correlated spin clusters that coexist with ferromagnetic metallic clusters and paramagnetic spins. This coexistence was found to be sensitive to the A -site disorder.

One of us, M.S.R. would like to acknowledge support by the Bundesminister für Bildung und Forschung (BMBF), Germany, within a joint Indo-German project.

*Also at Center for Superconductivity Research, Department of Physics, University of Maryland, College Park, Maryland 20742, USA. Electronic address: msrrao@iitm.ac.in

¹For a recent review, see *Colossal Magnetoresistive Materials*, edited by Y. Tokura (Gordon and Breach, New York, 2000).

²C. Zener, *Phys. Rev.* **82**, 403 (1951).

³A. Millis, P. Littlewood, and B. I. Shraiman, *Phys. Rev. Lett.* **74**, 5144 (1995).

⁴M. Jaime, M. B. Salomon, M. Rubinstein, R. E. Trece, J. Horwitz, and D. B. Chrisey, *Phys. Rev. B* **54**, 11 914 (1996).

⁵A. J. Millis, R. Mueller, and B. I. Shraiman, *Phys. Rev. B* **54**, 5405 (1996).

⁶J. M. De Teresa, R. Ibarra, P. A. Algarabel, C. Ritter, C. Marquina, J. Blasco, J. Garcia, A. del Moral, and Z. Arnold, *Nature (London)* **386**, 256 (1997).

⁷S. Yoon, H. L. Liu, G. Schollerer, S. L. Cooper, P. D. Han, D. A. Payne, S.-W. Cheong, and Z. Fisk, *Phys. Rev. B* **58**, 2795

(1998).

⁸M. Fath, S. Freisem, A. A. Menovsky, Y. Tomioka, J. Aarts, and J. A. Mydosh, *Science* **285**, 1540 (1999).

⁹E. Dagotto, H. Takashi, and A. Moreo, *Phys. Rep.* **344**, 1 (2001); see also **100**, 769 (1996).

¹⁰R. B. Griffiths, *Phys. Rev. Lett.* **23**, 17 (1969).

¹¹A. J. Bray and M. A. Moore, *J. Phys. C* **15**, L765 (1982).

¹²A. J. Bray, *Phys. Rev. Lett.* **59**, 586 (1987).

¹³M. B. Salamon, P. Lin, and S. H. Chun, *Phys. Rev. Lett.* **88**, 197203 (2002).

¹⁴V. Ravindranath, M. S. Ramachandra Rao, G. Rangarajan, Yafeng Lu, J. Klein, R. Klingeler, S. Uhlenbruck, B. Büchner, and R. Gross, *Phys. Rev. B* **63**, 184434 (2001).

¹⁵L. M. Rodriguez-Martinez and P. Attfield, *Phys. Rev. B* **54**, R15 622 (1996).

¹⁶H. Y. Hwang, S.-W. Cheong, P. G. Radaelli, M. Marezio, and B. Batlogg, *Phys. Rev. Lett.* **75**, 914 (1995).

- ¹⁷C. Rettori, D. Rao, J. Singley, D. Kidwell, S. B. Oseroff, M. T. Causa, J. J. Neumeier, K. J. McClellan, S.-W. Cheong, and S. Schultz, *Phys. Rev. B* **55**, 3083 (1997).
- ¹⁸P. Wagner, I. Gordon, L. Trappeniers, J. Vanacken, F. Herlach, V. V. Moshchalkov, and Y. Bruynseraede, *Phys. Rev. Lett.* **81**, 3980 (1998).
- ¹⁹S. L. Yuan, W. Y. Zhao, G. Q. Zhang, F. Tu, G. Peng, J. Liu, Y. P. Yang, G. Li, Y. Jiang, X. Y. Zeng, and C. Q. Tang, *Appl. Phys. Lett.* **77**, 4398 (2000).
- ²⁰J. Snyder, R. Hiskes, S. DiCarolis, M. R. Beasley, and T. H. Geballe, *Phys. Rev. B* **53**, 14 434 (1996).
- ²¹T. Holstein, *Ann. Phys. (N.Y.)* **8**, 343 (1959).
- ²²V. Kiryukhin, T. Y. Koo, A. Borissov, Y. J. Kim, C. S. Nelson, J. P. Hill, D. Gibbs, and S.-W. Cheong, *Phys. Rev. B* **65**, 094421 (2002).